

Giant Magnetic Moments and Magnetic Bistability of Stoichiometric MnO Clusters

S. K. Nayak* and P. Jena

Physics Department, Virginia Commonwealth University, Richmond, Virginia 23284-2000

(Received 29 May 1998)

Ab initio calculations based on density functional theory and generalized gradient approximation reveal many unusual features of stoichiometric $(\text{MnO})_x$ ($x \leq 9$) clusters that contrast with their bulk behavior. The clusters are ferromagnetic and carry atomlike magnetic moments ranging from $4\mu_B$ to $5\mu_B$ per MnO unit, and the moments are localized at the Mn sites. The $(\text{MnO})_8$ cluster, in particular, exhibits nearly degenerate ferromagnetic and atypical antiferromagnetic solutions with the ferromagnetic structure carrying a moment of $40\mu_B$. The structures of $(\text{MnO})_x$ clusters are also unique with cubic and hexagonal forms competing for stability. $(\text{MnO})_2$ and $(\text{MnO})_3$ are unusually stable and form the foundation for further growth. [S0031-9007(98)07121-X]

PACS numbers: 71.24.+q, 71.15.Mb, 75.50.Cc

The current interest in atomic clusters stems from the main observation that their properties are very different from the bulk [1]. One of these properties is associated with the unusual stability of clusters of a certain size and is evidenced by conspicuous peaks in the mass spectra [2–5]. The origin of these peaks, commonly referred to as magic numbers, depends on the chemistry of the elements [6]. For example, for weakly interacting species, such as rare-gas atoms, close packing of atoms gives rise to magic numbers as 13, 55, 143, ... (icosahedric shell closing) [3] while, for simple alkali metals, magic numbers at 2, 8, 20, ... are brought about by electronic shell closure [2]. For ionically bonded clusters such as alkali halides $(\text{NaCl})_x$ [4] and alkaline-earth oxides $(\text{MgO})_x$ [5], the magic numbers at $x = 4, 13, 22, 37, \dots$ can be understood as originating from the fcc structure of the bulk systems and by realizing that ultrastable clusters are fragments of their bulk. Transition metal-oxide clusters, on the other hand, not only exhibit different magic numbers [7] but also exist in compositions that differ from their bulk behavior. In particular, substoichiometric composition of these clusters, whether rich in metal or oxygen content, can render these oxide clusters unusual properties.

In this Letter we show that transition metal-oxide clusters having even the same composition as their bulk possess unusual structural, electronic, and magnetic properties. Their growth pattern is also unique, and structural isomers have rather markedly different magnetic properties. We illustrate this by carrying our first principles state-of-the-art calculations (with predictive capability) on small $(\text{MnO})_x$ ($x \leq 9$) clusters. These calculations, carried out for the first time, reveal that $(\text{MnO})_3$ is a magic cluster with $(\text{MnO})_2$ not too far behind, and that these two structures form the building blocks for the growth of larger clusters. The bonding between Mn and O is partly ionic, and the amount of charge transfer remains essentially the same in all clusters from the very beginning, namely, from the MnO molecule. The relative stability of the structural isomers is dictated by their underlying magnetic configuration. Isomers with a larger mag-

netic moment lie lower in energy than their counterpart with a smaller magnetic moment. All clusters, except $(\text{MnO})_8$, are ferromagnetic even though the bulk MnO is antiferromagnetic. The $(\text{MnO})_8$ cluster possesses nearly degenerate ferromagnetic and atypical antiferromagnetic solutions. The moments per MnO molecule in all of these clusters range between $4\mu_B$ and $5\mu_B$, and most of these moments are localized at the Mn site. The relative stability of the $(\text{MnO})_x$ clusters, as well as the bond distances and bond angles of smaller clusters, agree well with recent experiments. The predicted magnetic properties of these clusters, on the other hand, await experimental confirmation which should be relatively easy to perform.

We first discuss the available experimental results on $(\text{MnO})_x$ clusters. Ziemann and Castleman [7] have measured the mass spectra of these clusters for $x \leq 12$ and found $(\text{MnO})_x$ for $x = 3, 6, 9$, and 12 to be unusually stable. They suggested that the most likely structure of $(\text{MnO})_3$ is a hexagon and that subsequent stable clusters such as $x = 6, 9$, and 12 form by stacking the $(\text{MnO})_3$ hexagons on top of each other. They also observed that, under certain experimental conditions, the peak in the mass spectra corresponding to $(\text{MnO})_2$ is as intense as that of $(\text{MnO})_3$. They concluded that the larger clusters of $(\text{MnO})_x$ are formed by stacking $(\text{MnO})_3$ units in such a way that they are joined by a square $(\text{MnO})_2$ unit. Recently, Chertihin and Andrews [8] measured the infrared spectra of MnO and $(\text{MnO})_2$ clusters. Their suggested structure of $(\text{MnO})_2$ is, however, a rhombus with an estimated Mn-O and Mn-Mn bond distance of 2.0 and 2.6 Å, respectively, and the O-Mn-O bond angle of 99° [8]. No theoretical calculations on the geometries of $(\text{MnO})_x$ clusters are yet available to explain these apparently contradictory results.

We have calculated the equilibrium geometries, binding energies, electronic structure, and magnetic properties of $(\text{MnO})_x$ ($x \leq 9$) clusters using the molecular orbital theory. The atomic functions forming the molecular orbitals are taken as a double numerical basis with added polarization functions. The exchange-correlation

contribution to the potential is treated using the generalized gradient approximation prescribed by Perdew and Wang and Becke (BPW 91) within the framework of the density functional theory [9]. The calculations were carried out using the DMOL code [10]. This method yields the ionization potential of the Mn and O atoms to be 7.08 and 13.60 eV, respectively, which agree well with the corresponding experimental value of 7.43 and 13.62 eV [11]. The computed binding energy of 2.56 eV/atom and the bond length of 1.21 Å of the O₂ molecule also agree very well with the experimental value of 2.56 eV/atom and 1.21 Å [11]. The geometries of clusters up to (MnO)₃ are optimized without the use of any symmetry constraint. Different starting configurations were used to locate structures corresponding to both local and global minimum. The threshold for the forces at atomic sites was set to 10⁻⁶ a.u./Bohr. The geometries of smaller (MnO)_x ($x \leq 3$) clusters were used as an initial guess for optimizing the structures of larger clusters. For (MnO)₄ both planar and three-dimensional structures were probed by using C_{2h} and D_{2d} symmetry constraints, respectively. For (MnO)₆, we optimized the geometries by starting with two structures: a hexagonal-stacked structure (D_{3d} symmetry) with two (MnO)₃ hexagons joined together and a cubic structure (C_{2h} symmetry) consisting of three planes of (MnO)₂ units. The structure of (MnO)₈ was optimized with respect to C_2 symmetry. We explored the relative stability of both cuboid and hexagonal-stacked structures for (MnO)₉ subjected to C_{4v} and D_{3h} symmetry constraints. While optimizing the geometries, we found that there are isomers of these clusters that lie 0.5 to 2 eV above the lowest energy structure. In Fig. 1 we give only the geometries of (MnO)_x clusters corresponding to the lowest energy configuration. Details concerning low-lying isomers will be published elsewhere. In Table I we summarize the results of the binding-energy/MnO molecule, the average Mn-O bond distance, the average charge transfer from Mn to O and spin on the Mn and O atoms, and the total magnetic moment of the (MnO)_x clusters. The binding-energy/MnO molecule is defined as $E_b^x = E(\text{Mn}) + E(\text{O}) - E(\text{MnO})_x/x$. Here $E(\text{Mn})$, $E(\text{O})$, and $E(\text{MnO})_x$ are the total energies of the Mn atom, O atom, and (MnO)_x cluster, respectively. In the following we discuss the evolution of various properties of manganese-oxide clusters.

Atomic structure.—We begin with the equilibrium geometries of (MnO)_x clusters in Fig. 1. The calculated Mn-O distance in a MnO molecule of 1.65 Å agrees well with the experimental value of 1.78 Å [11]. The structure of (MnO)₂ is a rhombus with a Mn-Mn distance of 2.56 Å, O-O distance of 2.75 Å, and Mn-O distance of 1.88 Å. This is in agreement with the experimental result of Chertihin and Andrews [8] who estimated the Mn-Mn and Mn-O distances to be 2.6 and 2.0 Å, respectively. It is interesting to note that the bond distances of Mn₂ and O₂ are, respectively, 3.4 and 1.21 Å. Thus, in (MnO)₂

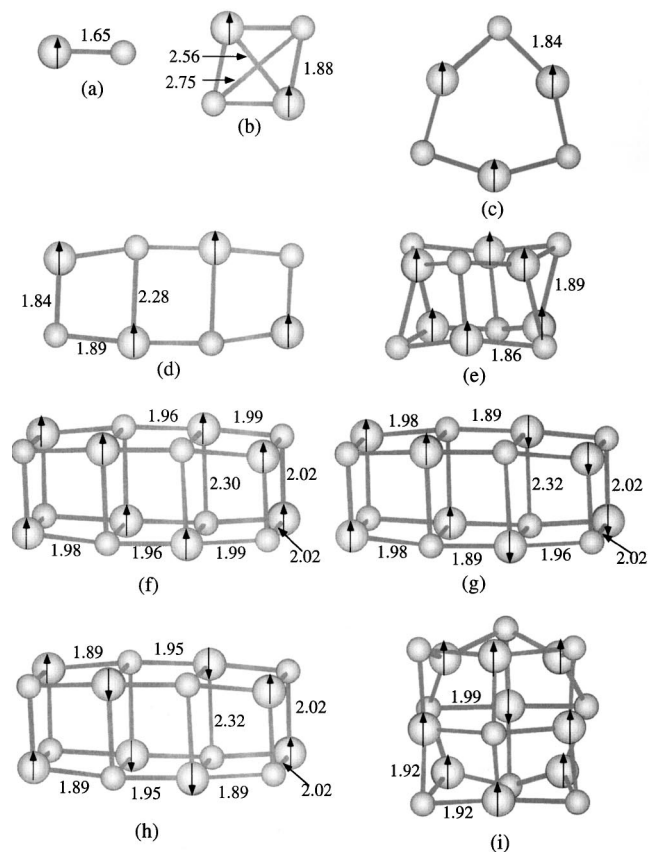


FIG. 1. Equilibrium geometries of (MnO)_x clusters ($x = 1-4, 6, 8, 9$). The Mn(O) atoms are represented by large (small) spheres. The arrows indicate the orientation of the electronic spin. For (MnO)₈ we give geometries corresponding to ferromagnetic and two antiferromagnetic configurations.

the metal-metal bond is stronger while the O-O bond is weaker than their homonuclear counterparts. The origin of this change is due to the electronic structure of MnO and will be discussed in the following. The structure of (MnO)₃ is hexagonal, as suggested by Ziemann and Castleman [7], and differs from what might have been ordinarily expected (namely, rectangular) based on its analogy with the bulk structure. The Mn-Mn bond is significantly smaller than the O-O bond, and, consequently, the structure of (MnO)₃ is not a perfect hexagon. The Mn-O bond in (MnO)₃ essentially remains the same as that in (MnO)₂. The geometry of (MnO)₄ still remains planar, but the Mn-O bond lengths vary from 1.84 to 2.28 Å. We recall that, in manganese acetate that consists of ligated Mn₁₂O₁₂ cluster, the Mn-O bonds have been measured to vary from 1.86 to 2.2 Å [12]. The Mn-O distance in bulk manganese oxide is 2.25 Å. Thus, the Mn-O bond lengths in free MnO clusters containing as few as four molecular units exhibit the crystalline behavior. Equally important is the observation that the ligands in manganese acetate do not seem to affect the Mn-O bond length. We will see in the following that this is due to the partly ionic nature of the Mn-O bond which makes binding in these clusters

TABLE I. Summary of the average Mn-O bond distance \bar{R}_e , charge transfer from Mn to O, \bar{Z} spin moments at Mn and O sites, $\bar{\mu}$, and the binding energy/MnO, E_b in $(\text{MnO})_x$ clusters.

Cluster size, X	Figure	\bar{R}_e (Å)	\bar{Z}	$\mu(\text{Mn})$ (μ_B)	$\mu(\text{O})$ (μ_B)	Total μ (μ_B)	E_b (eV)
1	1(a)	1.65	0.65	4.66	0.34	5.0	5.65
2	1(b)	1.88	0.81	3.89	0.11	8.0	6.91
3	1(c)	1.84	0.77	4.16	0.18	13.0	7.83
4	1(d)	1.99	0.79	4.73	0.27	20.0	7.88
6	1(e)	2.04	0.82	4.46	0.31	28.0	8.14
8	1(f)	2.07	0.84	4.71	0.29	40.0	8.43
8	1(g)	2.07	0.82	0.0	0.0	0.0	8.49
8	1(h)	2.07	0.82	0.0	0.0	0.0	8.52
9	1(i)	1.99	0.79	3.98	0.13	37.0	8.61

stronger. The geometry of $(\text{MnO})_4$ [Fig. 1(d)] suggests that $(\text{MnO})_2$ serves as a building block. This also carries to the structure of $(\text{MnO})_6$, where the equilibrium structure mimics the structure of its bulk. This lies 1.4 eV lower in energy than the optimized hexagonal-stacked structure, in contradiction with the suggestion of Ziemann and Castleman [7]. The structure of $(\text{MnO})_8$ is simply an extension of the $(\text{MnO})_6$ geometry with the addition of a $(\text{MnO})_2$ unit. Unlike the previous clusters, $(\text{MnO})_8$ has two other nearly degenerate isomers with similar geometries but with a very different magnetic character. It is important to note that once again the Mn-O bond distances vary between 1.89 and 2.3 Å, as observed to be the case in manganese acetate [12]. The structure of $(\text{MnO})_9$ appears to depart from the growth pattern discussed earlier, where the $(\text{MnO})_2$ unit is the building block. The preferred structure of $(\text{MnO})_9$ is a hexagonal-stacked structure with three $(\text{MnO})_3$ units stacked on top of each other. Its cubic counterpart lies energetically 1.44 eV above the hexagonal structure. The crystal structure of manganese acetate [12] that consists of $\text{Mn}_{12}\text{O}_{12}$ cluster as the building block reveals two different arrangements for MnO: a hexagonal structure of $(\text{MnO})_3$ and a rhombus structure of $(\text{MnO})_2$. The evolution of the structure of the gas phase $(\text{MnO})_x$ clusters bears this signature.

Stability and electronic structure.—The binding energy of MnO is 5.65 eV, which is significantly larger than the binding energy of Mn_2 (0.1 ± 0.1 eV) [13] or O_2 (5.12 eV) [11]. This arises because the Mn-O bond is partly ionic and is characterized by a charge transfer of 0.69 electrons from Mn to O. We see that in larger clusters this charge transfer remains nearly constant at 0.79 ± 0.02 . This indicates that the nature of bonding between Mn and O hardly changes from one cluster to another, which explains why the average Mn-O bond distance is insensitive to cluster size. The binding energy/MnO rises from 5.65 eV in MnO to 6.91, 7.83, 7.88, 8.14, 8.52, and 8.61 eV in $(\text{MnO})_x$ clusters ($x = 2, 3, 4, 6, 8,$ and 9), respectively. To evaluate the relative stability of these clusters, it is more meaningful to calcu-

late the energy gain in adding a MnO molecule to the preceding cluster, namely, $\Delta E_x = E(\text{MnO})_{x-1} - E(\text{MnO})_x$. For $x = 2, 3, 4$, the ΔE values are 8.16, 9.68, and 6.38 eV, respectively. This illustrates that $(\text{MnO})_3$ is relatively more stable than $(\text{MnO})_2$ or $(\text{MnO})_4$. This establishes $(\text{MnO})_3$ as a magic number and is in agreement with the mass spectra of Ziemann and Castleman [7]. Note that ΔE for $(\text{MnO})_2$ is also quite large. Thus, $(\text{MnO})_2$ and $(\text{MnO})_3$ form the building blocks for larger clusters. This is reflected in the geometries in Fig. 1 and in the structure of $\text{Mn}_{12}\text{O}_{12}$, as discussed earlier.

In addition to the partly ionic character of the Mn-O bond, the binding in the $(\text{MnO})_x$ cluster also has some covalent contribution. This is realized by analyzing the orbital character of the highest occupied molecular orbitals (HOMO). These are characterized by an overlap between O $2p$ electrons and hybridized $s-d$ electrons of Mn. This is further evidenced from an analysis of the deformed charge density (total cluster charge density-superimposed atomic charge density), which shows that charge is transferred from the Mn atoms to the O atoms. The charge around Mn is much more localized than that around O due to its $2p$ character. The bonding is due to the interaction of O $2p$ electrons with the hybridized $s-d$ electrons of Mn.

Magnetic properties.—The most exciting results in $(\text{MnO})_x$ clusters are, however, associated with their magnetic character. We recall that bulk MnO is antiferromagnetic [14] while nanoparticles of MnO are found to be ferromagnetic [15]. Clusters of $\text{Mn}_{12}\text{O}_{12}$ ligated to organic complexes have been found to exhibit an unusual form of magnetic ordering, where the inner four Mn atoms forming a tetrahedron exist in a Mn^{4+} state with $S = 3/2$ and the outer eight Mn atoms have Mn^{3+} configuration with $S = 2$ [12]. While the spins of the inner and outer shell of Mn atoms are parallel within the shell, they are antiparallel between the shells. The net magnetic moment of $\text{Mn}_{12}\text{O}_{12}$ acetate is $20\mu_B$ [12]. It is of interest to know how the moments at the Mn and O sites are aligned and how their coupling evolves with cluster size. Note that the magnetic moments of free Mn and O atoms are, respectively, $5\mu_B$ and $2\mu_B$. The calculated magnetic moment of the MnO molecule is $5\mu_B$ and agrees with the experimental value which is also $5\mu_B$. Of these moments, 93% are localized at the Mn site. We find this trend to hold as cluster sizes increase. All clusters studied here, with the exception of $(\text{MnO})_8$, are ferromagnetic, with moments ranging from $(4-4.6)\mu_B$ per MnO unit. More than 97% of these moments are localized at the Mn sites. The moments at the Mn sites arise due to the localized nature of the d electrons.

We now focus on the $(\text{MnO})_8$ cluster for it is the most interesting of all clusters we have studied here. It is the smallest cluster, where both ferromagnetic and antiferromagnetic solutions are nearly degenerate. In Figs. 1(f)–1(h) we have given the geometries corresponding to the ferromagnetic and two different antiferromagnetic

configurations; however, the antiferromagnetic couplings in Figs. 1(g) and 1(h) are rather unusual even though the geometries are the same for all three configurations. The only difference in geometry is associated with variations in the bond lengths. In the ferromagnetic phase [Fig. 1(f)] all of the Mn-O distances in the x - y plane are nearly the same. In Fig. 1(g), the Mn atoms in the central cube belonging to two $(\text{MnO})_2$ units are ordered antiferromagnetically and the Mn-O bond distance is slightly shortened. In Fig. 1(h), on the other hand, the moments at the Mn atoms belonging to two $(\text{MnO})_2$ units on the outer cubes are ordered antiferromagnetically while those in the central cube are ferromagnetic. The Mn-O distance in the cube, where Mn moments are antiferromagnetically aligned, is also shortened like that observed in Fig. 1(f). Note that the magnetic coupling in manganese acetate ($\text{Mn}_{12}\text{O}_{12}$) (ferromagnetic within the shell and antiferromagnetic between the shells) [12] is similar to the coupling in $(\text{MnO})_8$ in Fig. 1(h). In bulk MnO the antiferromagnetic coupling exists between nearest neighbor Mn atoms [14]. In this sense, the antiferromagnetic coupling in $(\text{MnO})_8$ shown in Figs. 1(g) and 1(h) is rather unusual. The energies of these three phases, interestingly, are very nearly the same as can be seen from Table I. The total moment of the ferromagnetic phase is $40\mu_B$. Thus, it is possible to change $(\text{MnO})_8$ from ferromagnetic to antiferromagnetic configuration with only minor changes in the bond distances.

The magnetic degeneracy in a $(\text{MnO})_8$ cluster is similar to that found in Mn clusters supported on a Ag(111) surface [16]. While the three isomers of $(\text{MnO})_8$ have very different magnetic character, the average Mn-O bond distance and Mulliken charge distribution are the same for all of the clusters. Thus, even though certain features (bond length and charge transfer) of $(\text{MnO})_x$ clusters have saturated even at small sizes, magnetically the clusters are very different from their bulk.

There are no experiments on the magnetic moments of small $(\text{MnO})_x$ clusters. However, using the same level of theory as discussed here, we have been successful in explaining the magnetic coupling in small Mn clusters isolated in rare-gas matrices [17]. Thus, we are confident

about the predictive capability of the theory used here. Since clusters of MnO are easily formed in the gas phase compared to clusters of Mn, it will be very useful if Stern-Gerlach experiments on $(\text{MnO})_x$ clusters can be performed to verify our prediction of ferromagnetism with rather large magnetic moments. In particular, a $(\text{MnO})_8$ cluster would be a particularly attractive candidate to study as it exhibits magnetic bistability.

This paper is supported in part by a grant from the Department of Energy.

*Present address: Princeton Materials Institute and Department of Chemistry, Princeton University, Princeton, New Jersey 08544.

- [1] See, e.g., the special issue on clusters, *Science* **271** (1996).
- [2] W.D. Knight *et al.*, *Phys. Rev. Lett.* **52**, 2141 (1984).
- [3] I.A. Harris, R.S. Kidwell, and J.A. Northby, *Phys. Rev. Lett.* **53**, 2390 (1984).
- [4] Y.J. Twu *et al.*, *Phys. Rev. B* **42**, 5306 (1990).
- [5] P.J. Ziemann and A.W. Castlemann, Jr., *J. Chem. Phys.* **94**, 718 (1991).
- [6] J.P.K. Doye and D.J. Wales, *Science* **271**, 484 (1996).
- [7] P.J. Ziemann and A.W. Castlemann, Jr., *Phys. Rev. B* **46**, 13 480 (1992); S. Veliah *et al.*, *Chem. Phys. Lett.* **235**, 53 (1995); *J. Phys. Chem. B* **102**, 1126 (1998).
- [8] G.V. Chertihin and L. Andrews, *J. Phys. Chem. A* **101**, 8547 (1997).
- [9] A.D. Becke, *Phys. Rev. A* **38**, 3098 (1988); J.P. Perdew and Y. Wang, *Phys. Rev. B* **45**, 13 244 (1992).
- [10] DMOL Code, Biosym Technologies, San Diego, 1995.
- [11] G. Herzberg, *Spectra of Diatomic Molecules* (Van Nostrand, New York, 1979).
- [12] R. Sessoli *et al.*, *J. Am. Chem. Soc.* **115**, 1804 (1993).
- [13] M.D. Morse, *Chem. Rev.* **86**, 1049 (1986).
- [14] P.A. Cox, *Transition Metal Oxides, An Introduction to their Electronic Structure and Properties* (Clarendon Press, Oxford, 1992).
- [15] J. Li *et al.*, *Appl. Phys. Lett.* **70**, 3047 (1997).
- [16] V.S. Stepanyuk *et al.*, *Surf. Sci. Lett.* **384**, L892 (1997).
- [17] S.K. Nayak and P. Jena, *Chem. Phys. Lett.* **289**, 473 (1998); M.R. Pederson, F. Reuse, and S.N. Khanna (unpublished).